COULOMB SCATTERING CROSS SECTIONS FOR ACCELERATOR DESIGN

M.N. Butler, S. Koscielniak, G.H. Mackenzie and F. Jones

TRIUMF, 4004 Wesbrook Mall, Vancouver, B.C., Canada V6T 2A3

Abstract

The commonly used models to estimate the Coulomb scattering in the thin foils used for charge exchange injection are barely adequate for the new and proposed intense spallation neutron sources and kaon factories. The modification to the Rutherford cross section due to the screening from the electronic shells has been calculated by an iterative Hartree-Fock method for cases of interest to accelerator designers. These include Be, C, Al and O foils over an energy range 0.025 to 1.6 GeV. The differential and total cross sections are compared with earlier models. The best fit to a Thomas-Fermi model for each case is also given for convenient substitution into existing programs and calculations. Some practical examples of the effect on accumulated phase space distributions and beam loss are given for proton accumulation at 450 MeV.

Introduction

Spallation neutron sources and the proposed hadron facilities store or accelerate $\sim 10^{15}$ p/s (~ 100 μA). Charge exchange injection is the most efficient process for accumulating beam over many turns in a circular machine. While this process leads to a higher central brightness than few turn positive ion inflection, it also creates halos or tails by angular scattering and energy loss in the charge exchange medium. The tails can lead to beam loss either directly, by subsequent growth in betatron amplitude-dependent resonances, or by mismatch into and resonant growth in following accelerator stages. Calculations[1] and experience[2] indicate that losses of 0.1% to 0.5% may be associated with foil interaction processes. A quantitative estimate is important since meson factory experience shows that the use of regular materials and routine hands-on maintenance require losses ≤ 1 nA/m. Radiation-resistant materials and quasi-remote handling may be used for losses ≤ 10 nA/m (0.01% of 100 μA). Losses of more than 0.2 μA/m in one location require radiation-hard materials and full remote handling.

Injection energies range from 0.07 to ~ 1 GeV. Stripper thicknesses $\sim 10^{-4}$ g/cm^2 are required for efficient conversion to H$^+$. The average number of scattering events for a stored proton traversing the medium lies between 1 and 20, i.e. in the plural scattering regime.

The literature shows some variation in the treatment of plural scattering, both in the magnitude of the Coulomb scattering cross section and in its application. Multiple scattering models have been tested experimentally; however, there seems little data on plural scattering in this regime. The Rutherford law well describes the scattering of protons by a point Coulomb field. For large impact parameters, small angles of scatter, however, the screening effect of the atomic electrons causes the Coulomb potential to fall off more rapidly than an inverse square. Methods of modifying the scattering potential are reviewed by Scott.[3] The more precise methods are not analytically tractable and the discrepancies between theoretical treatments arise from different analytic approximations.

The total scattering cross section σ_t determines the average number, n, of scattering events per proton traversing a foil thickness t; $n = N\sigma_t t$, where N is the atomic density. Variations in shape of the differential cross section have only a small effect on the final rms betatron amplitude since this approximates the sum of the rms amplitude of an unscattered accumulated beam, σ_0, and the rms scattering amplitude σ_n.[4] Usually $\sigma_n < \sigma_0$. The halo distributions, however, are dominated by foil interaction

processes since it is assumed that an unscattered beam has no tails. Also since the injected emittance is smaller than the ring acceptance the foil is usually placed towards the outer edge of the ring acceptance. This minimizes the number of foil traversals. It means, however, that relatively small angles of scatter may take the particles outside the acceptance and form a halo.

It was decided, therefore, to make more accurate calculations of single scattering from proposed target materials in the energy range of interest for existing and proposed synchrotron injection. The emerging distribution from a foil would be obtained by numerical rather than analytic methods. The first step was to calculate the charge distribution around a given nucleus to greater accuracy; the second was to calculate the differential and total cross sections and the third to convolve these to describe plural scattering.

Calculations

Atomic Charge Distribution

The configuration of atomic electrons is determined by the Coulomb interaction of the electrons with the nucleus and with each other. The latter depends, however, on the electron configuration. The Hartree-Fock approach is an iterative procedure which evolves the system from some simple starting configuration until a self-consistent solution is reached. Existing Hartree-Fock codes (MNB) for both atoms and nuclei have been adapted to calculate charge distributions. Spherical symmetry and the most simple distribution of particles in shells is assumed for both the atomic and the nuclear densities. A typical net charge distribution is compared with a result from a Thomas-Fermi calculation in Fig. 1. The shell structure is apparent and there is a difference in the tails of the distributions.

Single Scattering

The differential cross section ($d\sigma/d\Omega$) for elastic Coulomb scattering from the overall potential of individual, isolated atoms was calculated using relativistic kinematics. Any distortions in the charge distributions due to inter-atomic forces were ignored. Ionization, excitation and other inelastic collisions were not included; these contribute to energy loss but the scattering angle is small. Strong interaction scattering only becomes important
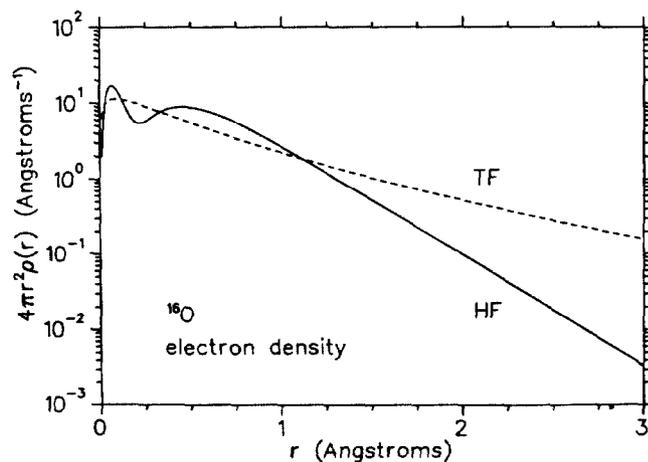
Fig. 1. Comparison of Thomas Fermi model and Hartree-Fock calculations of charge density.
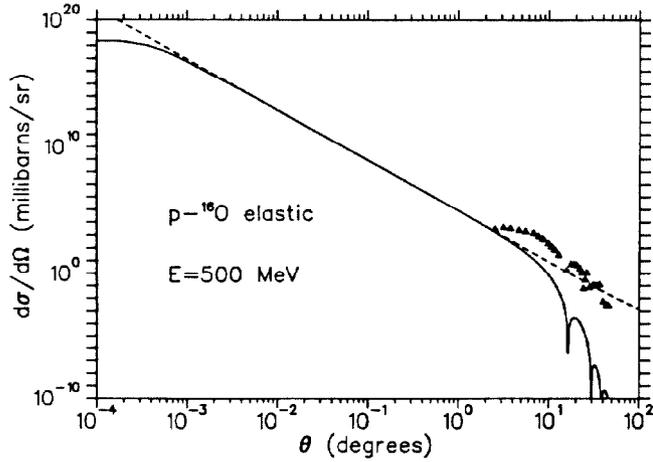
Fig. 2. Differential cross section versus laboratory angle for Coulomb scattering. The triangles are measurements of nuclear elastic scattering plus Coulomb scattering. The dashed line is the Rutherford formula for an unscreened point charge.

at angles which would lead to immediate beam loss; the effect on the halo distribution is negligible. This loss may be estimated from tabulations of total nuclear cross section. The calculated differential cross section for ^{16}O is compared with measurements[5] including nuclear elastic scattering in Fig. 2. The experimental data appear to blend smoothly with the pure Coulomb curve but some interference effects may still occur at smaller angles. Inelastic events maintain the overall cross section at ~10 mb/sr at large angles. Also shown is the unscreened Rutherford cross section.

The cross section with respect to polar angle, θ, is

$$d\sigma/d\theta = 2\pi \sin\theta (d\sigma/d\Omega) \equiv f(\theta)\sigma_t \ , \qquad (1)$$

and the total cross section, σ_t, is the integral of $(d\sigma/d\theta)$ from 0 to π. Since the integral of $f(\theta)$ between 0 and π is unity, then $f(\theta)d\theta$ is the probability that a single scattering event will deflect a particle between θ and $\theta + d\theta$. The cumulative density function $F(\theta)$ is the integral of $f(\theta)$ between 0 and θ. The inverse of $F(\theta)$ maps random numbers in the range [0,1] into scattering angles distributed according to $f(\theta)$. The cross section and related parameters are, in general, not analytic and the angle generator must, in turn, employ look up tables, interpolations or other numerical techniques.

An Approximation for Single Scattering

A convenient analytic approximation for the screened Coulomb potential is[3]

$$V(r) = (zZe^2/r) \exp(r/a) \ , \qquad (2)$$

where $a \approx \mu a_0 Z^{1/3}$ represents an effective atomic radius and a_0 is the Bohr radius. Thomas-Fermi model calculates a value for μ of 0.885; Jackson[6] prefers a value of 1.4 as better describing a general range of atomic and ionic calculations. In the small angle approximation

$$\begin{aligned}
\left.\frac{d\sigma}{d\theta}\right|_A &= \left(\frac{2\theta \cdot \theta_{min}^2}{(\theta^2 + \theta_{min}^2)^2}\right)\sigma_t \\
\left.\sigma_t\right|_A &= 4\pi(zZe^2/pv)/\theta_{min}^2 \\
F_A(\theta) &= \theta^2/(\theta^2 + \theta_{min}^2) \ , \qquad (3)
\end{aligned}$$

where θ_{min} is a cut-off angle approximated $\theta_{min} \approx \hbar/pa \approx Z^{1/3}/(ka_0)$ and the subscript A means "approximate" and if a generator G returns random numbers uniform in the range [0,1], then the angle generator is $\theta = \theta_{min}[G/(1-G)]^{1/2}$. Note

that the cross sections depend on the square of the arbitrary scale factor μ.

Suitable μ may be calculated from fits to the numerically calculated cross section. From typical values of beam emittance and machine acceptance and also bearing in mind that the probable number of foil traversals in a workable high intensity machine is less than or equal 10^3/proton the fit for these applications was most heavily weighted in the angular range 10^{-4}–10^{-2} rad. Note that the differential cross section gives the angular distribution of protons undergoing a scattering event. The number of such events is determined by σ_t. This is best calculated by numerical integration. It will not, however, be $\int_0^\pi (d\sigma/d\theta)_A d\theta$. This does not matter for the applications discussed herein. However, a self-consistent approach requires a fit to both differential and total cross sections. Table I gives values of θ_{min} for both cases. Note that θ_{min} for ^{27}Al is less than that for ^{16}O, a consequence of the electronic shell structure. Figure 3 shows the influence of μ on the angular region of best fit.

Plural Scattering

Since the average number of scatters per traversal $n \ll Nt$ the probability of a particular proton undergoing m events on one traversal is $(n^m e^{-n})/m!$ Earlier authors[3,7] obtained the angular distribution after m scatters by sequentially folding analytic expressions for the single scattering distribution m times. The final distribution is the probability-weighted sum for all m. The results were often tabulated for values of n in the plural scattering regime.

A more convenient numerical approach has been used by Thiessen.[8] The average distance travelled in the material before scattering events, the collision length, is $\lambda = A/(N_0\sigma_i\rho)$ where A is the atomic weight, N_0 is Avogadro's number and ρ the density. The probability density function for a distance x between successive collisions is

$$P(x)dx = (1/\lambda) \exp(-x/\lambda)dx \ . \qquad (4)$$

Random calls to $\ln P(x)$ return values of x populating a Poisson distribution. A series of such calls are made when a particle is assumed to have entered the stripping medium. After each call i a test is made that $\Sigma x_i < t$. If this is satisfied a call is made to the angle generator. The angle of scatter for the emerging particles is $\Sigma \theta_i$. It has been confirmed that the two approaches yield identical results.
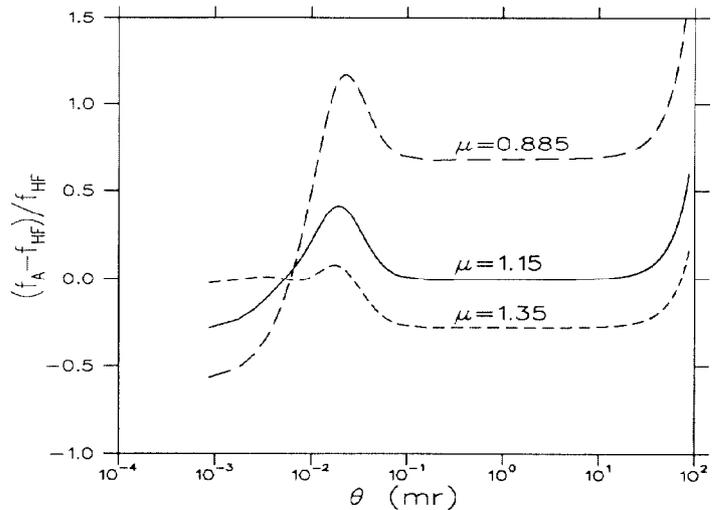
Fig. 3. Difference between the approximate scattering probability f_A and the Hartree-Fock calculation f_{HF} for 450 MeV protons on ^{12}C. A scaling parameter choice $\mu = 1.35$ best fits the cross-section peak, $\mu = 1.15$ fits the region $0.1 < \theta < 1.0$ mrad, $\mu = 0.885$ is the classic Thomas-Fermi model value. A single precision random number generator forms an effective large angle cut-off at ~20 mV.

655

Table I. Total cross section σ_t and parameter θ_{min} from fit to function (Eq. 3), given as a function of the incident proton kinetic energy.

Energy (MeV)	^{9}Be σ_{tot} (Mb)	^{9}Be θ_{min} (μrad)	^{12}C σ_{tot} (Mb)	^{12}C θ_{min} (μrad)	^{16}O σ_{tot} (Mb)	^{16}O θ_{min} (μrad)	^{27}Al σ_{tot} (Mb)	^{27}Al θ_{min} (μrad)
25	2.904	18.16	4.898	23.02	4.824	34.43	10.34	24.51
50	1.545	12.74	2.625	16.12	2.658	23.93	5.738	17.03
75	1.079	10.34	1.837	13.07	1.877	19.38	4.072	13.80
100	.8437	8.895	1.437	11.25	1.475	16.67	3.208	11.88
150	.6060	7.173	1.033	9.070	1.065	13.44	2.323	9.575
200	.4866	6.136	.8303	7.760	.8577	11.50	1.873	8.192
250	.4150	5.423	.7084	6.858	.7328	10.16	1.601	7.240
300	.3673	4.891	.6273	6.188	.6495	9.170	1.419	6.532
350	.3334	4.476	.5695	5.666	.5901	8.394	1.290	5.980
400	.3081	4.135	.5263	5.241	.5456	7.765	1.193	5.532
425	.2977	3.987	.5086	5.058	.5274	7.492	1.153	5.338
450	.2885	3.849	.4929	4.889	.5112	7.242	1.118	5.159
475	.2803	3.722	.4789	4.734	.4968	7.011	1.087	4.995
500	.2729	3.604	.4664	4.591	.4839	6.798	1.058	4.843
600	.2498	3.120	.4269	4.110	.4432	6.079	.9694	4.333
700	.2335	2.875	.3991	3.736	.4144	5.518	.9068	3.937
800	.2215	2.608	.3786	3.434	.3933	5.064	.8606	3.620
900	.2123	2.442	.3629	3.184	.3771	4.687	.8252	3.361
1000	.2051	2.311	.3506	2.971	.3643	4.367	.7973	3.146
1100	.1993	2.183	.3407	2.764	.3541	4.092	.7749	2.967
1200	.1945	2.053	.3326	2.603	.3457	3.852	.7565	2.814
1300	.1906	1.939	.3258	2.462	.3387	3.639	.7413	2.685
1400	.1872	1.836	.3201	2.336	.3328	3.449	.7284	2.574
1500	.1844	1.743	.3153	2.225	.3278	3.279	.7175	2.450
1600	.1820	1.658	.3111	2.123	.3235	3.124	.7081	2.398

Application

Numerical calculations were made using a Monte Carlo program ACCSIM modified to exhibit only Coulomb scattering effects. 450 MeV protons repeatedly traverse a 250 μg/cm^2 carbon foil. The situation represents a possible stage in the accumulation of charge for the TRIUMF KAON Factory. The particles are centred in longitudinal and vertical phase space but occupy an annulus in radial phase space. The tune values, $Q_x = 5.793$, $Q_y = 5.739$, are such that on average an unscattered particle traverses the foil on about 0.8% of the turns. The particle motion is followed using first-order optics including only Coulomb scattering; space charge forces, chromatic effects and the effect of energy loss have not been incorporated. Calculations were made for the same models used for Fig. 3.

Acknowledgements

References

[1] A.A. Kaminsky, R.A. Mescherov and M.I. Popova, Nucl. Instrum. Meth. **137**, 183 (1976).

[2] R.J. Macek, D.H. Fitzgerald, R.L. Hutson, M.A. Plum and H.A. Thiessen, submitted to PAC Rome, 1988.

[3] W.T. Scott, Rev. Mod. Phys. **35**, 231 (1963).

[4] R.K. Cooper and G.P. Lawrence, IEEE Trans. **NS-22**, 1916 (1975).

[5] C.K-K. Chan, MSc. thesis, Univ. of Alberta, 1985 (unpublished).

[6] J.D. Jackson, Classical Electrodynamics (Wiley, New York, 1962) and private communication.

[7] E. Keil, E. Zeitler and W. Zinn, Naturforsch. **15a**, 1031 (1960).

[8] H.A. Thiessen, LAMPF II Technical Note 85-007.